Available online at www.sciencedirect.com
SCIENCE DIRECT®
Chemical Physics 317 (2005) 119–129
Chemical Physics
www.elsevier.com/locate/chemphys

LDA or GGA? A combined experimental inelastic neutron scattering and ab initio lattice dynamics study of alkali metal hydrides

G.D. Barrera [a,b], D. Colognesi [c], P.C.H. Mitchell [d], A.J. Ramirez-Cuesta [a,d,*]

[a] ISIS Facility, Rutherford Appleton Laboratory, Chilton, Didcot, Oxon OX11 0QX, UK
[b] Departamento de Química, Universidad Nacional de la Patagonia SJB, Ciudad Universitaria, 9005 Comodoro Rivadavia, Argentina
[c] Consiglio Nazionale delle Ricerche, Istituto dei Sistemi Complessi, via Madonna del Piano s.n.c., 50019 Sesto Fiorentino (FI), Italy
[d] School of Chemistry, University of Reading, RG6 6AD, UK

Received 3 February 2005; accepted 25 April 2005
Available online 14 June 2005

Abstract

In a previous work, we carried out inelastic neutron scattering (INS) spectroscopy experiments and preliminary first principles calculations on alkali metal hydrides. The complete series of alkali metal hydrides, LiH, NaH, KH, RbH and CsH was measured in the high-resolution TOSCA INS spectrometer at ISIS. Here, we present the results of ab initio electronic structure calculations of the properties of the alkali metal hydrides using both the local density approximation (LDA) and the generalized gradient approximation (GGA), using the Perdew–Burke–Ernzerhof (PBE) parameterization. Properties calculated were lattice parameters, bulk moduli, dielectric constants, effective charges, electronic densities and inelastic neutron scattering (INS) spectra. We took advantage of the currently available computer power to use full lattice dynamics theory to calculate thermodynamic properties for these materials. For the alkali metal hydrides (LiH, NaH, KH, RbH and CsH) using lattice dynamics, we found that the INS spectra calculated using LDA agreed better with the experimental data than the spectra calculated using GGA. Both zero-point effects and thermal contributions to free energies had an important effect on INS and several thermodynamic properties.

Keywords: Inelastic neutron scattering; Alkali metal hydrides; Hydrogen storage materials; DFT calculations; Free energy calculations; Thermodynamic properties; INS spectra; Abinitio calculations; LiH; NaH; KH; RbH; CsH; Bulk modulus

1. Introduction

Alkali metal hydrides are of interest as model systems with the simplest anion and cations in the periodic table, but as potential hydrogen storage materials. Like the alkali metal halides, the alkali metal hydrides crystallize with the rock-salt structure. With the exception of LiH, these hydrides were found to transform to the CsCl structure at high pressures [1,2]; LiH is predicted to change its structure [3] but only at very high pressures ($P \sim 660$ GPa).

In spite of the difficulty of growing single crystals of high-purity LiH because of its reactivity towards atmospheric gases, LiH and LiD have been the subject of several experimental studies. Dispersion curves of LiD obtained from neutron scattering experiments [4], and complementary vibrational information for LiH obtained from Raman spectroscopy [5], structural information [6–9] and elastic data [10] are available.

Lithium hydride and deuteride have been also the subject of extensive theoretical investigations using atomistic simulations and ab initio electronic structure methods. The most successful atomistic simulations on LiH and LiD are those of Verble et al. [4] who proposed a seven parameter shell model (model IV). With this

* Corresponding author. Tel.: +44 1235446510.
E-mail address: a.j.ramirez-cuesta@rl.ac.uk (A.J. Ramirez-Cuesta).

0301-0104/$ - see front matter © 2005 Elsevier B.V. All rights reserved.
doi:10.1016/j.chemphys.2005.04.027

model, it is possible to reproduce satisfactorily the experimental dispersion curves. Their model did not, however, reproduce the experimental elastic constants, C_{ij}, for instance the calculations predicted $C_{12} = 30.4$ GPa, while the experimental value at room temperature is 14.7 GPa [10]. Another limitation of these calculations was the use of an axially symmetric second neighbour model with parameters restricted only by symmetry. The parameters of the model are not distance dependent and so it is not possible to consider the effects of temperature or pressure on the calculated properties. To overcome this last limitation, Haque and Islam [11] proposed a shell model with interatomic potentials of the form (Buckingham potential)

$$\varphi_{ij}(r) = B_{ij}\exp(-\alpha_{ij}/r) - \frac{D_{ij}}{r^6}, \tag{1}$$

where B_{ij}, α_{ii}, and D_{ij} are constants that depend on the type of ions (i,j) and r is the distance between them. For the NaCl structure, the shell model implies that the Cauchy relation be obeyed, viz. $C_{12} = C_{44}$. Experimental data [10] for LiH ($C_{12} = 14.2$ GPa, $C_{44} = 48.4$ GPa) show that for LiH the Cauchy relation is not obeyed. A correct description of elastic properties is essential to reproduce properly the thermal behaviour at low temperatures [12]. The incorporation of many body forces could improve the quality of the potentials allowing a correct reproduction of experimental dispersion curves and elastic data, but bonding in LiH is clearly more covalent than in the analogous alkali metal halides indicating that more investigation on atomistic models is necessary.

First principles electronic structure calculations of LiH have been more successful than atomistic simulations in providing a quantitative description of its phonon spectra and derived elastic and thermal properties. Roma et al. [13] carried out ab initio simulations of LiH using the local density approximation (LDA) and the plane wave pseudo-potential method. Their calculated dispersion curves were in good agreement with the experimental data of Verble et al. [4] and clearly showed the importance of taking into account zero-point effects. The bulk modulus, for instance, decreases by approximately 10% when zero-point effects are taken into account, compared with the value obtained in the static approximation. Bellaiche et al. [14] have shown that electron correlation does *not* play an important role in the determination of the equation of state of LiH – a consequence of the small number of electrons in LiH.

We have recently reported the inelastic neutron scattering (INS) spectra of the complete series of alkali metal hydrides: LiH, NaH, KH, RbH and CsH [15], and calculated their spectra ab initio [16]. Except for LiH there has been no previous experimental study on the lattice dynamics of the alkali metal hydrides. In a computational study of the lattice dynamics of the hydrides other than LiH, Dick and Jex [17] developed a shell model with force constants derived from those of LiD and shell parameters obtained from the ion polarizabilities. Haque and Islam [11] used a different shell model to calculate the dispersion curves of LiH, LiD, NaH and NaD. The calculations were carried out in the static approximation, and so neglected zero-point contributions. Islam et al. [18] used their potential to calculate elastic constants for lithium and sodium hydrides and deuterides and their pressure and temperature dependence [19]. Experimental and theoretical work on Li, Na and K hydrides has been reviewed [20]. These various models use a shell model with pair potentials and hence require $C_{12} = C_{44}$. The failure of the Cauchy relation for LiH ($C_{12}/C_{44} \approx 0.3$) leads one to enquire whether the relation should be obeyed by the other hydrides. No doubt the inclusion of three body forces would improve these potentials [21], but the lack of experimental data would make parameter fitting difficult.

With our experimental INS spectra, we reported the spectra calculated ab initio using density functional theory within the LDA approximation [16] and lattice dynamics. For all alkali metal hydrides, we found excellent agreement between the experimental and calculated INS spectra. The calculated dispersion curves of ^{7}LiH were found also in good agreement with experiment. There are no experimental phonon dispersion curves for the other alkali metal hydrides. The good agreement between the experimental and computed INS spectra gave us the incentive and confidence to calculate properties for the family of alkali metal hydrides. In this paper, we present the results of our calculations and compare with experiment. As a check of the computational procedure, we have now used both the LDA and the generalized gradient approximation GGA, using the parameterization of Perdew, Burke and Ernzerhof (PBE) functional [22]. Vibrational contributions have been taken into account explicitly using lattice dynamics within the quasi-harmonic approximation and their relative importance is also discussed. Properties calculated were lattice parameters, bulk moduli, INS spectra, Born effective charges, dielectric constants and electron densities.

2. Theoretical methods

In the quasi-harmonic approximation [23], it is assumed that the Helmholtz energy of a crystal, F, at temperature T is the sum of static and vibrational contributions

$$F = E_{\text{stat}} + F_{\text{vib}}(T). \tag{2}$$

Here, E_{stat} is the potential energy of the static lattice in a given configuration and F_{vib} is the sum of the harmonic vibrational contributions from the normal modes. For a

periodic structure, the frequencies $\omega_j(\mathbf{q})$ are obtained by diagonalizing the dynamical matrix [24], so that F_{vib} is given by

$$F_{\text{vib}} = \sum_{j=1}^{3N} \sum_{\mathbf{q}} \left(\frac{1}{2}\hbar\omega_j(\mathbf{q}) + kT \ln\left(1 - e^{\hbar\omega_j/kT}\right) \right), \tag{3}$$

where the first term is the zero-point energy at $T = 0$ and the second term is the thermal contribution. For a macroscopic crystal, the sum over $\mathbf{q}$ becomes an integral over a cell in reciprocal space, which can be evaluated by taking successively finer uniform grids until convergence is achieved. Vibrational frequencies do not depend on temperature explicitly, but do so implicitly through the position of the atoms in the unit cell, which determines the dynamical matrix. The free energy obtained is a function of both some external coordinates, $\mathscr{R}^{\text{ext}}$, which are here taken as the lattice parameters (a for a cubic crystal, a and c for a hexagonal crystal, etc.) and a set of internal coordinates which give the position of the atoms within the unit cell $\mathscr{R}^{\text{int}} = \{r\}$; this whole set of coordinates is denoted collectively as $\mathscr{R}$. For a given temperature and applied pressure, P_{ext}, the crystal structure is that which minimizes the availability $\tilde{G}$ [25]

$$\tilde{G}(\mathscr{R}) = F(\mathscr{R}) + P_{\text{ext}} V(\mathscr{R}^{\text{ext}}). \tag{4}$$

At the equilibrium configuration, $P = P_{\text{ext}}$ and the availability equals the Gibbs energy

$$\tilde{G} = G \equiv F + PV. \tag{5}$$

An efficient method to minimize $\tilde{G}$ is described elsewhere [26]. For crystals with the NaCl structure, there are no internal degrees of freedom and so the free energy depends only on the lattice parameter a.

Here, it is important to emphasize the difference between static calculations, calculations at 0 K, and at finite temperature, for instance 298 K. Static calculations assume that atoms are fixed at their equilibrium positions, which are determined by minimizing the static energy E_{stat}. Vibrational contributions are not included. Calculations at $T = 0$ K require the evaluation of phonon frequencies and the minimization of $E_{\text{stat}} + \sum_{j=1}^{3N} \sum_{\mathbf{q}} \frac{1}{2}\hbar\omega_j(\mathbf{q})$. The difference between static and 0 K calculations involves the zero-point energy contribution $\sum_{j=1}^{3N} \sum_{\mathbf{q}} \frac{1}{2}\hbar\omega_j(\mathbf{q})$. Although still commonly used in the literature, it is misleading to use the expression "calculations at 0 K" when referring to static calculations. Calculations at finite temperature involve the minimization of $E_{\text{stat}} + \sum_{j=1}^{3N} \sum_{\mathbf{q}} \frac{1}{2}\hbar\omega_j(\mathbf{q}) + kT \ln(1 - e^{\hbar\omega_j/kT})$, including both the zero-point energy and the thermal contribution $kT \ln(1 - e^{\hbar\omega_j/kT})$.

Our calculations were carried out using plane wave density functional theory as implemented in the computer code Abinit [27]. Here, there are two main approximations. The first approximation is the use of *pseudo-potentials* to represent the core electrons, allowing one to include relativistic effects in a mainly non-relativistic code, and to reduce the number of planes waves necessary to represent the wavefunction to a number tractable with available computer power. The second approximation is inherent in the use of density functional theory. In the LDA the exchange and correlation energies depends on the local density on each point in space. In the generalized gradient approximation (GGA), electron density gradients are taken into account to determine the exchange and correlation energies [28].

In our earlier paper, we reported the INS spectra of all alkali metal hydrides calculated using LDA [16]. However, because it has been proposed that, GGA gives results on average, although not uniformly, in better agreement with experiment than does LDA [29], we have now carried out our calculations using both LDA and GGA. The LDA calculations were done using the Teter–Padé parameterization [30]; the GGA calculations were based on the parameterization of Perdew, Burke and Ernzerhof. We used the Hartwigsen–Goedecker–Hutter pseudo-potentials (HGH) [31].

We have verified that convergence is achieved with respect to the number of k-points in reciprocal space and energy cutoff for the plane waves. Most calculation were done using a mesh of $4 \times 4 \times 4$ points in reciprocal space and a cutoff of 50 Ha. The calculation of effective charges and dielectric constants required a mesh of $8 \times 8 \times 8$ point in reciprocal space to give converged values [32]. Phonon frequencies were calculated on the same grid of points of reciprocal space used for the electronic structure calculations and the interpolation algorithm of Gonze as implemented in the anaddb code [33]. From the phonon frequencies, free energies and derived thermodynamic properties were determined using standard lattice dynamics calculations in the quasi-harmonic approximation as described above.

The intensity, S, of an INS spectral band is a function of both the energy, $\hbar\omega$, and the momentum, $\mathbf{Q}$, exchanged during the scattering process. Recalling that $|\mathbf{q}| = 2\pi/\lambda$ and $Q = |\mathbf{Q}|$, from the conservation of energy and momentum, we have

$$\mathbf{Q} = \mathbf{q}_{\text{scattered}} - \mathbf{q}_{\text{incident}}, \tag{6}$$

$$\begin{aligned} \hbar\omega = E_{\text{tranf}} &= E_{\text{incident}} - E_{\text{scattering}} \\ &= \frac{\hbar^2}{2m_n} \left(|\mathbf{q}_{\text{incident}}|^2 - |\mathbf{q}_{\text{scattering}}|^2 \right), \end{aligned} \tag{7}$$

where $\mathbf{q}_{\text{incident}}$ and $\mathbf{q}_{\text{scattered}}$ are the momentum of the neutron before and after the scattering process and E_{incident} and $E_{\text{scattering}}$ are the corresponding kinetic energies of the neutron. Because of the geometry of the TOSCA instrument [34], the final energy of the instrument is fixed to be 32 cm^{-1}. Because of the relatively large momentum transfer in the TOSCA measuring range;

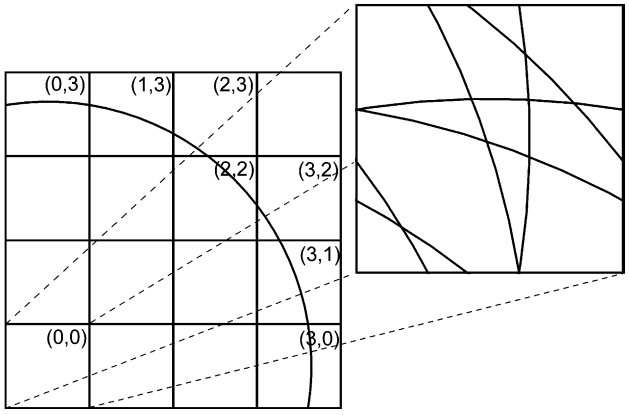

Fig. 1. A two-dimensional representation of the momentum transfer in a polycrystalline system; the circle represents a Q value of 3.1 zone widths. The width of the Brillouin zone for LiH corresponds to about 1.5 $Å^{-1}$.

the projection of the momentum transfer maps uniformly into the first Brillouin zone [35], see Fig. 1.

The intensity of an INS band, S_α, produced by atom α when vibrating at a frequency ω_i with amplitude U_i is

$$S_\alpha(Q, n\omega_i) = \frac{(Q \cdot U_i)^{2n}}{n!} \exp(-(Q \cdot U_T)^2) \cdot \sigma_\alpha \quad (8)$$

where $n = 1$ for a fundamental mode, 2 for a first overtone or binary combination, 3 for a second overtone or ternary combination, and so forth; Q is the momentum transfer defined before, σ_α is the scattering cross section of atom α, U_i is the amplitude of the normal mode i and U_T is the total root-mean-square displacement of the α atom in all the modes, both internal and external.

For a periodic solid, the solution of the vibrational problem contains a dependency with the wavevector in reciprocal space, the intensity is now

$$S_\alpha(Q, n\omega_i) = \frac{1}{V_{\text{Brillouin}}} \int \frac{(Q \cdot U_i(\mathbf{q}))^{2n}}{n!} \exp(-(Q \cdot U_T)^2) \cdot \sigma_\alpha \, d\mathbf{q}^3. \quad (9)$$

The integration has to be performed over the whole Brillouin zone; $V_{\text{Brillouin}}$ is the volume of the Brillouin zone. In order to calculate the INS spectra of the alkali metal hydrides, we need a fine grid of points in the Brillouin zone, we used a $16 \times 16 \times 16$ grid to obtain well-defined INS spectra. We do not need to undetake a full electronic calculation in such a grid, instead we make use of the anaddb program from the Abinit package. The INS spectra were generated using the aClimax program [36].

3. Results

To visualize the effects of lattice vibrations, we show the calculated properties for the alkali metal hydrides series calculated using LDA and GGA in the so-called static approximation and, after considering temperature effects, using the quasi-harmonic approximation of lattice dynamics.

In Table 1, we show the values of the lattice parameters calculated for alkali metal hydrides in the static approximation and using quasi-harmonic lattice dynamics at temperatures of 20 K and 298 K using both LDA and GGA; we also show the room temperature experimental values of the lattice parameters [37–43].

The calculated bulk moduli for all alkali metal hydrides calculated in the static limit and at 20 K and 298 K using quasi-harmonic lattice dynamics are given in Table 2, together with room temperature experimental data [44,45].

Table 1
Calculated and room temperature experimental lattice parameters (Å) of the alkali metal hydrides

	LDA			GGA			Experiment
	Static	QH (20 K)	QH (298 K)	Static	QH (20 K)	QH (298 K)	RT
LiH	3.938	4.017	4.038	4.025	4.112	4.142	4.084[a] 4.0856[b] 4.0752[c] 4.0835[d]
NaH	4.738	4.835	4.855	4.869	4.937	4.976	4.89[e]
KH	5.469	5.541	5.581	5.692	5.768	5.835	5.704[f]
RbH	5.793	5.862	5.907	6.047	6.134	6.198	6.037[g]
CsH	6.105	6.167	6.219	6.429	6.505	6.584	6.388[h]

Calculated values at finite temperatures include vibrational contributions.
[a] See [9].
[b] See [37].
[c] See [38].
[d] See [39].
[e] See [40].
[f] See [41].
[g] See [42].
[h] See [43].

Table 2
Calculated and room temperature experimental bulk modulae (GPa) of the alkali metal hydrides

	LDA			GGA			Experiment
	Static	QH (20 K)	QH (298 K)	Static	QH (20 K)	QH (298 K)	RT
LiH	40.5	35.8	33.3	36.2	31.9	28.8	32.2[a] 31.9[b]
NaH	27.2	23.6	22.6	24.0	22.5	20.2	14.3 ± 1.5[c] 19.4 ± 2.0[e]
KH	17.4	15.2	12.4	13.4	12.4	10.1	15.6 ± 1.5[c]
RbH	14.7	13.1	10.7	11.1	9.72	9.08	10.0 ± 1.0[c]
CsH	11.9	10.6	9.5	9.0	8.5	8.1	7.6 ± 0.8[c] 8.0 ± 0.7[d]

Calculated values at finite temperatures include vibrational contributions.
[a] See [9].
[b] See [44].
[c] See [1].
[d] See [45].
[e] See [2].

3.1. Lattice parameters

In Fig. 2, we represent the errors in the determination of the lattice parameters in accordance with Table 1. In the static approximation, Fig. 2(a), the agreement between the calculated and experimental lattice parameters is better when using the GGA functional; the lattice parameters calculated using the LDA functional are underestimated by 3–5%.

The effect of the phonon contribution can be seen by comparing Fig. 2(a) and (b). While the inclusion of zero-point vibrational contributions improves the agreement of the LDA calculations of the lattice parameters it worsens the agreement of the GGA calculations. When temperature effects are now included in the calculations, Fig. 2(c), the overall picture changes: LDA calculations of the lattice parameters are slightly better than GGA when compared with experiment. Still the LDA calculations underestimate the lattice parameters while the GGA calculations overestimate the lattice parameters.

3.2. Bulk moduli

In Fig. 3(a), we show the errors in percent of the experimental and calculated values of the bulk moduli for the static approximation. The agreement between

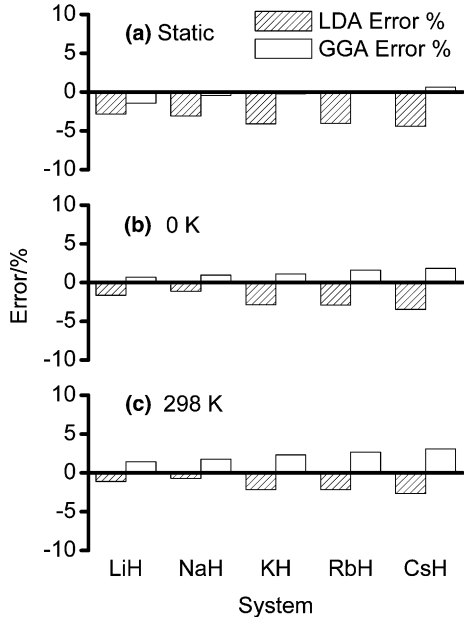

Fig. 2. Errors in percent of the calculated lattice parameter for the series of alkali metal hydrides: (a) in the static approximation, where no dynamical effects are considered, (b) zero-point effects are included, and (c) zero-point effects as well as temperature effects are included.

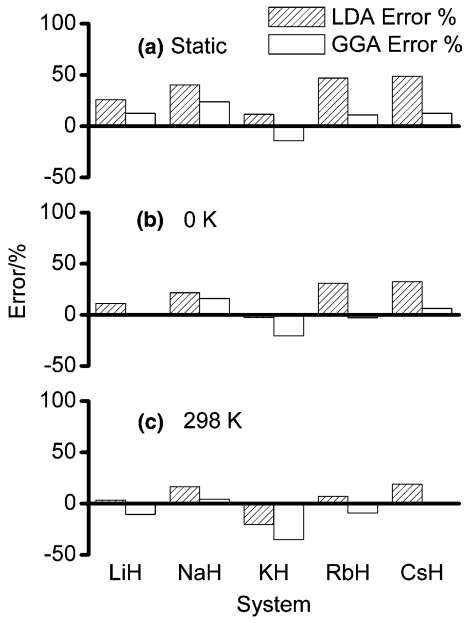

Fig. 3. Errors in percent of the calculated bulk moduli for the series of alkali metal hydrides: (a) in the static approximation, where no dynamical effects are considered, (b) zero-point effects are included, and (c) zero-point effects as well as temperature effects are included.

experiment and theory is not good, since errors over 40% are found. In the static approximation, the calculated bulk moduli are better for the GGA functional except for KH, where the LDA calculation performs marginally better.

In Fig. 3(b), when zero-point effects are taken into consideration, GGA calculations show a marked improvement with the experimental bulk moduli, although LDA calculations also improve the agreement with the experiment.

In Fig. 3(c), temperature effects are included and the comparison with experiment should be more realistic. In this case, LDA calculations perform slightly better overall than GGA calculations. Although major conclusions cannot be made, we emphasize that new measurements of the bulk moduli are required.

The effect of vibrations (at 0 K) is now comparatively larger than that shown by lattice parameters and change from static values by more than 10%. Neither LDA nor GGA is better on the values of the bulk moduli obtained from the calculations. However, the discrepancies may well reflect the uncertainties in the experimental data (see Table 2). The actual experimental errors for CsH, for instance, may be larger that those quoted in Table 2 as the bulk modulus determined by Hochheimer et al. [1] was determined from only three points of the V/V_0 vs. P curve, while Ghandehari et al. [45] were forced to assume a value of the bulk modulus pressure derivative of 4.0 due to the insufficient number of data to fit a first order Birch equation. In passing, we note that our calculations provide further support for the bulk modulus of NaH determined by Duclos et al. [2] in comparison to that reported by Hochheimer et al. [1].

3.3. Effective charges and dielectric constants

The calculation of effective charge tensors $\mathbf{Z}_i^*$ as implemented in the abinit [27] code has been described in detail by Ghosez et al. [46]. For the rock-salt structure adopted by the alkali metal hydrides $\mathbf{Z}_i^*$ is a diagonal matrix with all equal diagonal elements (Z^*). By symmetry, $Z_{\mathrm{M}}^* = -Z_{\mathrm{H}}^*$, where Z_{M}^* and Z_{H}^* are the effective charges of the cation and anion, respectively. The value of Z_i^* represents the rigid ion charge needed to produce the actual polarization resulting by an infinitesimal displacement of the ion. A formal definition and comparison with other atomic charge definitions have been given by Ghosez et al. [46], where it is also explained how covalence effects can produce Z_i^* values greater than one.

The calculated charges are shown in Table 3 [47]; experimental data are available only for LiH. Our calculated value for LiH ($Z_{\mathrm{Li}}^* = 1.043$ using LDA and $Z_{\mathrm{Li}}^* = 1.038$ using GGA) are in good agreement with the experimental value of Brodsky and Burstein [47] ($Z_{\mathrm{Li}}^* = 0.99 \pm 0.04$) and the calculations of Blat et al. [48] ($Z_{\mathrm{Li}}^* = 1.06$) and Shukla [49] ($Z_{\mathrm{Li}}^* = 1.046$). The calculated values for NaH are also in good agreement with the result of Blat et al. ($Z_{Na}^* = 0.99$). The values of Z_i^* for the different hydrides obtained using GGA are always slightly larger than those obtained from LDA calculations and all are close to the formal charge of $Z_i^* = 1$.

Table 3
Calculated and experimental Born effective charges at 298 K

	LDA	GGA	Experiment
LiH	1.043	1.038	0.99 ± 0.04[a]
NaH	0.974	0.990	
KH	0.975	1.004	
RbH	1.034	1.049	
CsH	1.139	1.119	

[a] See [47].

In Table 4, we show the calculated values of the low and high frequency limits of the frequency-dependent dielectric constant. In the low frequency limit, when both ions and electrons can respond to the applied electric field, the dielectric constants (ε_0) obtained from LDA calculations are systematically lower that those obtained using GGA. On the contrary, in the high frequency limit, when only electrons can respond to the applied electric field, the dielectric constants obtained from LDA calculations are systematically higher than those obtained using GGA.

3.4. INS spectra simulation

In Fig. 4, we show the INS spectra measured on TOSCA together with the result of our calculations using both LDA and GGA. The arrows indicate the energy transfer limit for contributions from the fundamental transitions; at higher frequencies the spectral intensities are due to overtones and combinations. In these calculations, we used the quasi-harmonic approximation and optimized the lattice parameters including the vibrational effect at $T = 20$ K, the temperature at which INS experiments were carried out. For all five alkali metal hydrides, the spectra obtained from LDA simulations are in much better agreement with experiment than those obtained from GGA simulations. This, in turn strongly suggests that vibrational and in general

Table 4
Calculated and experimental dielectric constants for the alkali metal hydrides at 298 K

	LDA		GGA		Experiment	
	ε_0	ε_∞	ε_0	ε_∞	ε_0	ε_∞
LiH	16.34	4.92	18.53	4.28	12.9 ± 0.5[a]	3.61[a]
NaH	9.87	3.35	10.47	3.12		
KH	8.06	2.94	10.16	2.69		
RbH	8.66	3.07	10.99	2.73		
CsH	9.83	3.45	12.65	2.98		

[a] See [47].

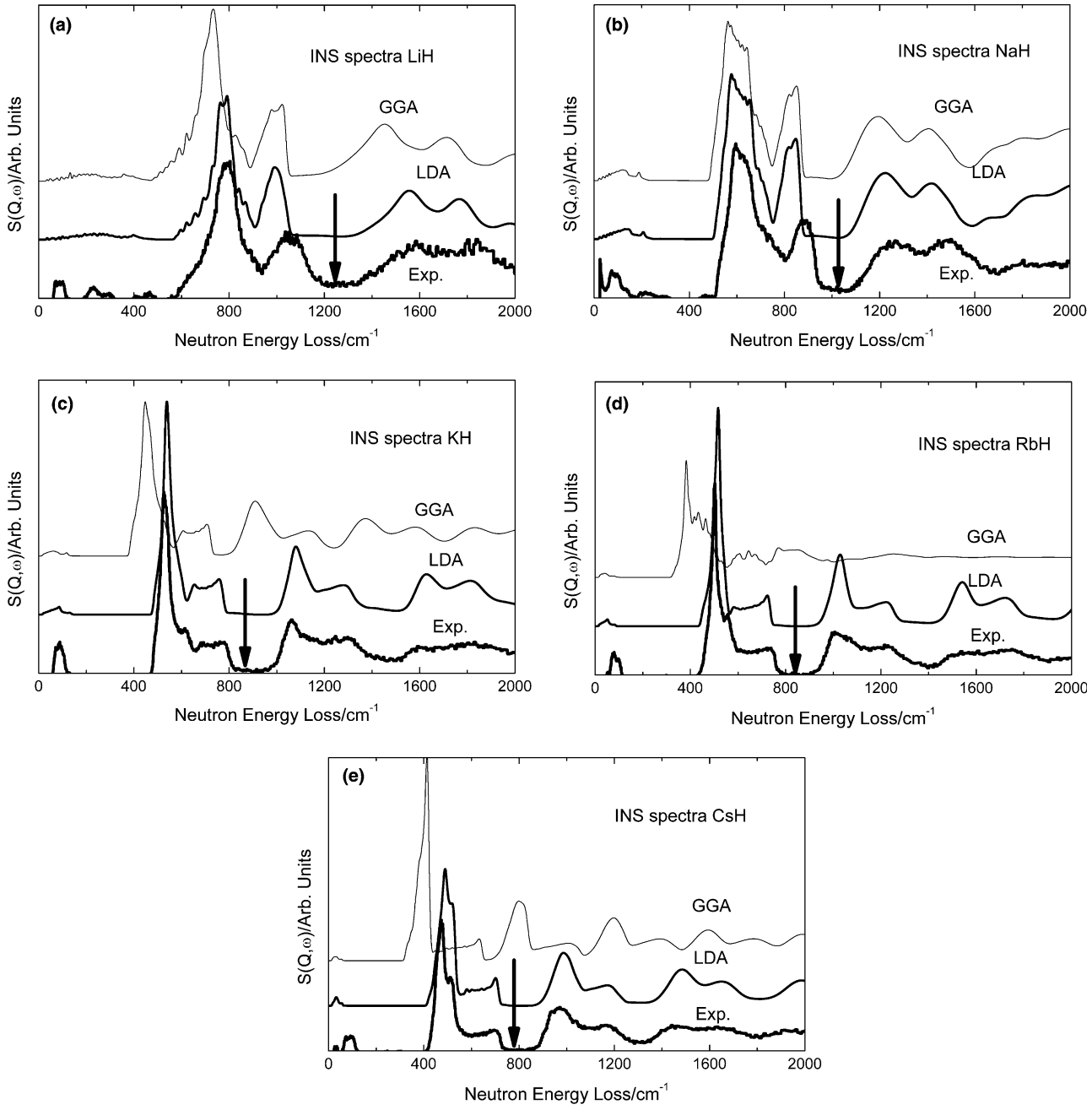

Fig. 4. INS spectrum of: (a) LiH, (b) NaH, (c) KH, (d) RbH, and (e) CsH determined from LDA and GGA calculations using quasi-harmonic lattice dynamics at $T = 20$ K, and from experimental data.

dynamical properties of these solids are better described by LDA than by GGA calculations.

As the primitive cell contains two atoms, dispersion curves show in general six branches: three acoustic and three optical. For all alkali metal hydrides, the acoustic branches appear below 400 cm^{-1}. The optical branches correspond to two transversal branches (TO) and one longitudinal (LO) branch. As a more compact, but rather less informative, way of representing the quality of the calculated results, we can use the position of the centre of mass of the main peak (TO). The comparison of the calculations at $T = 20$ K using LDA and GGA using this compact form is shown in Fig. 5, where we plot the percentage difference within calculated and experimental positions of the main TO peak.

To study the importance of taking into account vibrational contributions in calculating lattice parameters (i.e., the effect of vibrations on thermal expansion) and their effect on the INS spectra, we have repeated the simulations using the lattice parameters obtained in the static limit and using quasi-harmonic lattice dynamics at $T = 20$ K using LDA. Instead of showing

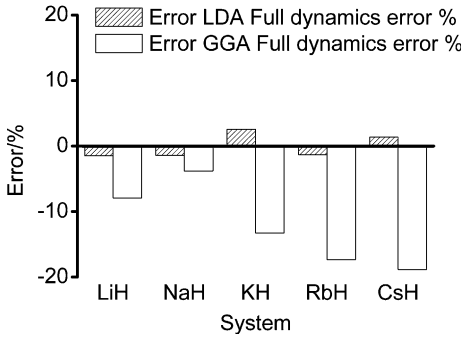

Fig. 5. Percentage difference of the calculated position of the centre of mass main peak (TO mode) with respect to experiment for alkali metal hydrides. Ab initio calculations were carried out fully dynamically at $T = 20$ K including both zero point and thermal effects.

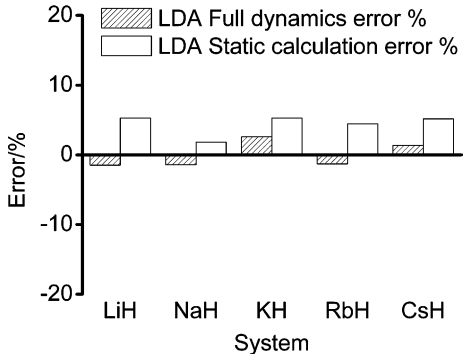

Fig. 6. Percentage difference of the calculated position of the centre of mass main peak (TO) with respect to experiment for all alkali metal hydrides. Ab initio calculations were carried out in the static limit and fully dynamically at $T = 20$ K including both zero-point and thermal effects.

the calculated and experimental spectra for all alkali metal hydrides, we resort to a more compact plot similar to that presented in Fig. 5. In Fig. 6, we show the difference between the experimental and calculated, using LDA, main peaks both in the static approximation and at $T = 20$ K. The agreement of the spectra calculated using lattice parameters in the static limit with the experimental data is much poorer than that obtained from lattice parameters calculated using the quasi-harmonic approximation at $T = 20$ K. The spectra obtained from simula-

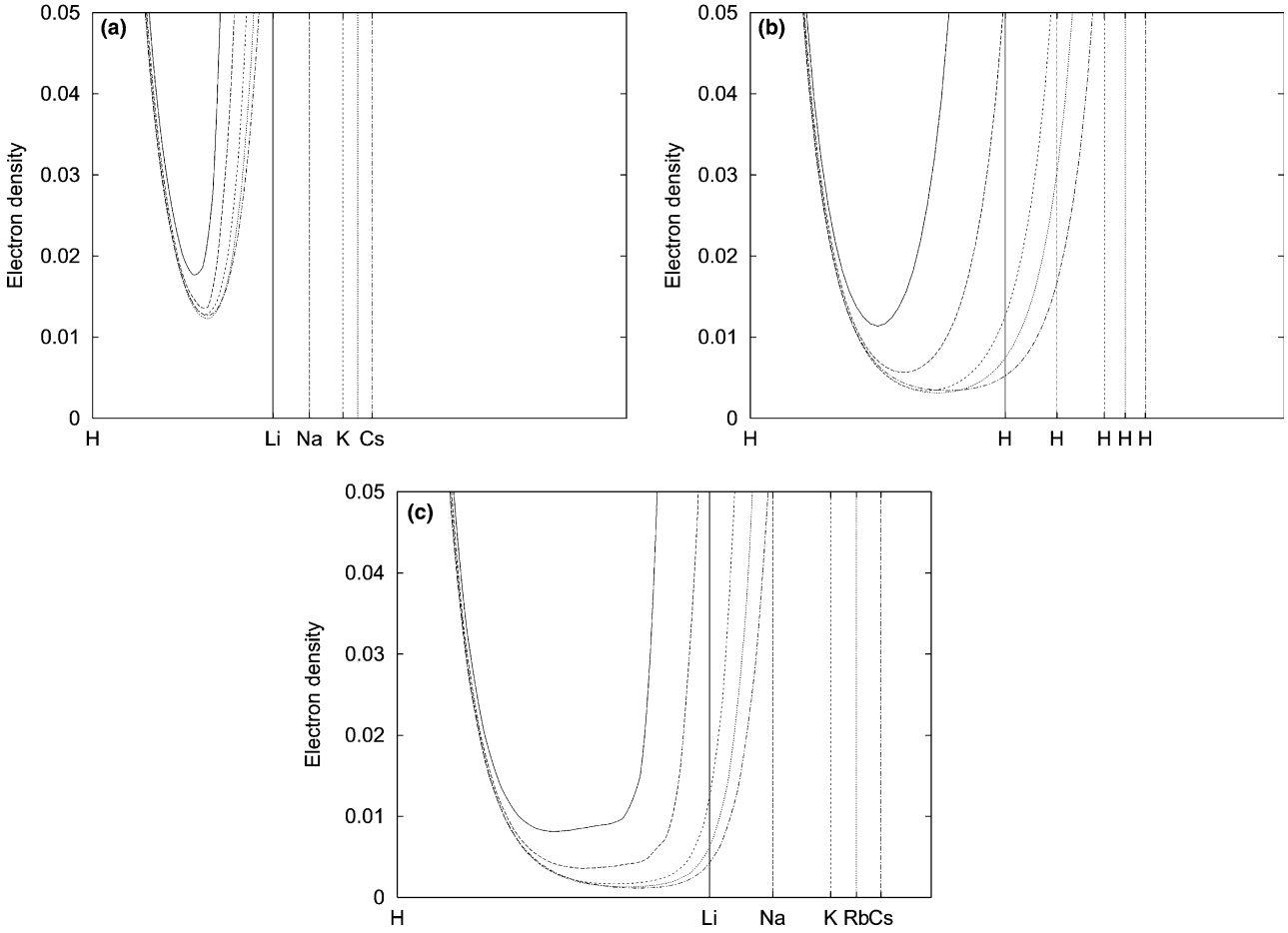

Fig. 7. Electron density as a function of distance calculated from LDA simulations in the static limit along three different directions: (a) (1 0 0), (b) (1 1 0), and (c) (1 1 1). In all cases, a H atom is located at the origin; vertical lines indicate the distance where a nearest neighbour along each direction is found. Vertical lines, from left to right correspond to LiH, NaH, KH, RbH and CsH. All plots use the same scale.

tions using the lattice parameters calculated at $T = 298$ K, not shown here, also show a poorer agreement with experiment than that obtained from simulations at 20 K, though the discrepancy is not so large. We see that for the simulation of INS spectra and the calculation of lattice parameters it is crucial to take vibrational contributions and temperature effects into account.

3.5. Electron density and elasticity

In Fig. 7, we show the electron density as a function of distance along three directions. In all cases, a hydrogen atom is located at the origin. Along the (1 0 0) direction (Fig. 7(a)) there is an alkali metal nearest neighbour at $a/2$. Next nearest neighbours, hydrogen atoms, are found along the (1 1 0) direction (Fig. 7(b)) at $\frac{\sqrt{2}}{2}a$, and second cation nearest neighbours are found along the (1 1 1) direction (Fig. 7(c)) at $\frac{\sqrt{3}}{2}a$. The minimum electron density along the nearest neighbour direction, Fig. 7(a), is at approximately 1.48 Å for LiH and at values ranging from 1.63 to 1.66 Å for the other alkali metal hydrides. The electron density at the minimum is approximately 0.0177 electron/Bohr [3] for LiH and ranges from 0.0136 to 0.0126 electron/Bohr [3] for the other hydrides. This suggests that the hydrogen anion is smaller in LiH than in the other hydrides, where it has an approximately constant size. This is consistent with the more covalent character of the H-metal bond in LiH compared to the other hydrides as expected from the higher polarization power of the Li^+ ions. In all three directions shown in Fig. 7 there is a higher interionic electron density in LiH than in the other hydrides. Potassium, rubidium and caesium hydrides show a very similar electron density, with NaH being intermediate between these and LiH.

The relatively more covalent bonding in LiH can also be inferred from the Cauchy violation in the elastic constants. If only two body forces were responsible for the bonding in theses solids, the quotient C_{12}/C_{44} should be close to 1. In sodium chloride, a typical example of ionic bonding the value is 1.09. For LiH C_{12}/C_{44} is 0.20 (Table 5), while for NaH, KH and RbH the value is 0.6. The calculated value for CsH is $\approx$0.25.

Because of computer power limitations, we were able to calculate the elastic constants for the alkali metal hydrides only in the static approximation, neglecting the effect of vibrations. Mainly as a consequence of experimental difficulties in growing single crystals, experimental values for the elastic constants are limited to LiH [10]. The room temperature experimental values are $C_{11} = 67.2$, $C_{12} = 14.8$ and $C_{44} = 46.1$ GPa. While these values differ somewhat from than those calculated here (100.9, 10.3 and 51.4 GPa), the main reason could be the neglect of vibrational effects in the calculations. For comparison, the bulk modulus calculated in the static approximation (40.5 GPa) is appreciably larger that that calculated using quasi-harmonic lattice dynamics at 298 K (33.3 GPa), which is then in good agreement with the experimental value of 32.2 GPa.

Table 5
Elastic constants calculated in the static approximation

	C_{11}	C_{12}	C_{44}
LiH	100.9	10.3	51.4
NaH	56.9	15.9	24.7
KH	39.4	6.3	10.4
RbH	35.1	4.5	7.6
CsH	33.4	1.2	4.7

4. Conclusions

In this paper, we have presented properties of the alkali metal hydrides (LiH, NaH, KH, RbH and CsH) obtained from ab initio calculations, using two different functionals and including vibrational contributions. Previous theoretical and experimental work was summarized to show that, for this system, atomistic models like the shell model are not suitable for describing even qualitatively the elasticity and thermal behaviour of these materials.

Ab initio calculations were carried out using HGH pseudo-potentials and plane waves as implemented in the code abinit and considering both LDA and GGA functionals. For these systems, the crystal structure is completely determined by the lattice parameter a. In the static approximation, i.e. neglecting the contribution of phonons to the free energy, lattice parameters calculated using GGA are in good agreement with available room temperature experimental data while those calculated using LDA underestimate the experimental values by over 4%. The inclusion of vibrational effects, however, makes an important contribution to the free energies, even at 0 K, and increases the calculated values of the lattice parameters. The finite temperature contribution to the free energy (obtained from fully dynamical optimizations) allows the proper comparison of the experimental and calculated properties. Lattice parameters calculated using LDA and fully dynamical optimization are in good agreement with the experimental data while values calculated using GGA appreciably overestimate the experimental values.

A similar situation occurs with the calculated bulk moduli. In the static approximation, values calculated using LDA overestimate available room temperature experimental data; whereas values calculated using GGA show a better agreement with the experiment. The incorporation of vibrational effects, by performing fully dynamic optimization, decreases the calculated bulk moduli improving the agreement of the calculations using LDA, which are now, overall, in better agreement with experiment than those using GGA.

LiH gives a striking example of the importance of vibrational contributions: while the experimental bulk modulus of LiH is 32.2 GPa, the values calculated using LDA in the static approximation and including vibrational contributions are 40.5 and 33.3 GPa. The neglect of vibrational contribution would lead, at least for this system, to a large overestimate of the bulk modulus.

The effective charges calculated using both LDA and GGA are in all cases close to the formal value of 1, with values obtained using GGA sometimes slightly higher than those calculated using LDA. However, and in spite of the high formal charges of these ions, the bonding has important covalent contributions, as evidenced from the deviations of the Cauchy relations and the electronic density maps. For NaCl, a typical example of ionic bonding $C_{12}/C_{44} \approx 1.09$ while for the series LiH to CsH the values calculated using LDA in the static approximation are 0.20, 0.64, 0.61, 0.59 and 0.26. Vibrational contributions are unlikely to appreciably change the quotient C_{12}/C_{44}. It is worth remembering that atomistic models with two body forces only, give $C_{12}/C_{44} = 1$ [21], and deviations from this value only arise when three or many body forces are considered. From the electronic density plots given in Fig. 7, it was shown that the hydrogen anion is comparatively smaller in LiH than in the other hydrides, due to the higher polarizing power of the Li^+ ions. From the plots given in Fig. 7, it can also be seen that the electronic density as a function of distance from a hydrogen atom strongly depends on the direction, a characteristic feature of covalent bonding.

We have also calculated the INS spectra for the whole series of alkali metal hydrides using both LDA and GGA. If the phonon spectra are calculated using lattice parameters obtained in the static approximation, GGA results show a better agreement with experiment than those obtained from LDA calculations. However, when fully dynamic calculations are carried out, LDA performs systematically better than GGA. It is worth stressing that temperature effects, included in lattice dynamics through quasi-harmonic calculations, are not negligible and should always be included.

Although LDA calculations show a better agreement with experiment when fully dynamic calculations are carried out it is worth noting that calculations using *GGA in the static approximation* show also a very good agreement with the experiment. Though for the alkali metal hydrides the simple NaCl structure (where only one parameter needs to be optimized) has allowed us to carry out extensive ab initio lattice dynamic calculations this may not be the case for more complicated solids. For crystals with more complicated structures, free energies have to be minimized with respect to several lattice parameters and internal coordinates. Computer time may make the calculations unfeasible and so GGA calculations in the static approximation could be considered as an approximate alternative. Of course, more theoretical work in this area is required before making more general conclusions.

Acknowledgements

G.D.B. acknowledges support from the Consejo Nacional de Investigaciones Científicas y Técnicas de la República Argentina and the Centre for Molecular Structure and Dynamics. Ab initio results have been obtained through the use of the ABINIT code, a common project of the Université Catholique de Louvain, Corning Incorporated, and other contributors (URL: http://www.abinit.org). Useful discussions with Prof. N.L. Allan (University of Bristol) and Dr. Keith Refson (ISIS, Rutherford Appleton Laboratory) are greatly appreciated. A.J.R.-C. acknowledges the award of a Visiting Fellowship in the University of Reading and P.C.H.M. a Leverhulme Emeritus Fellowship.

References

[1] H.D. Hochheimer, K. Strossner, W. Honle, B. Baranowski, F. Filipek, Z. Phys. Chem. 143 (1985) 139.
[2] S.J. Duclos, Y.K. Vohra, A.L. Ruoff, Phys. Rev. B 36 (1987) 7664.
[3] G. Li, D. Wang, Q. Jin, D. Ding, Phys. Lett. A 143 (1990) 473.
[4] J.L. Verble, J.L. Warren, J.L. Yarnell, Phys. Rev. 168 (1968) 980.
[5] A.C. Ho, R.C. Hanson, A. Chizmeshya, Phys. Rev. B 55 (1997) 14818.
[6] E. Staritsky, D. Walker, Anal. Chem. 28 (1956) 1055.
[7] G. Vidal-Valat, J.P. Vidal, Acta Crystallogr., Sect. A 48 (1992) 46.
[8] J.M. Besson, G. Weill, G. Hamel, R.J. Nelmes, J.S. Loveday, S. Hull, Phys. Rev. B 45 (1992) 2613.
[9] P. Loubeyre, R. Le Toullec, M. Hanfland, L. Ulivi, F. Datchi, D. Hausermann, Phys. Rev. B 57 (1998) 10403.
[10] B.W. James, J. Kheyrandish, J. Phys. C 15 (1982) 6321.
[11] E. Haque, A.K.M.A. Islam, Phys. Stat. Sol. (b) 158 (1990) 457.
[12] T.H.K. Barron, G.K. White, Heat Capacity and Thermal Expansion at Low Temperatures, Kluwer Academic, New York, 1999.
[13] G. Roma, C.M. Bertoni, S. Baroni, Solid State Commun. 98 (1996) 203.
[14] L. Bellaiche, J.M. Besson, K. Kunc, B. Lévy, Phys. Rev. Lett. 80 (1998) 5576.
[15] D. Colognesi, A.J. Ramirez-Cuesta, M. Zoppi, R. Senesi, T. Abdul-Redah, Physica B 350 (2004) E983.
[16] G. Auffermann, G.D. Barrera, D. Colognesi, G. Corradi, A.J. Ramirez-Cuesta, M. Zopi, J. Phys. 16 (2004) 5731.
[17] W. Dyck, H. Jex, J. Phys. C 14 (1981) 4193.
[18] A.K.M.A. Islam, E. Haque, A.S. Azad, Phys. Sat. Sol. (b) 183 (1994) 117.
[19] A.K.M.A. Islam, M.T. Hoque, J. Phys. Soc. Jpn. 65 (1996) 3557.
[20] A.K.M.A. Islam, Phys. Stat. Sol. (b) 180 (1993) 9.
[21] M.B. Taylor, N.L. Allan, J.A.O. Bruno, G.D. Barrera, Phy. Rev. B 59 (1999) 353.
[22] J.P. Perdew, K. Burke, M. Ernzerhof, Phys. Rev. Lett. 77 (1996) 3865.
[23] D.C. Wallace, Thermodynamics of Crystals, Wiley, New York, 1972.

[24] N.L. Allan, G.D. Barrera, R.M. Fracchia, M. Yu Lavrentiev, M.B. Taylor, I.T. Todorov, J.A. Purton, Phys. Rev. B 63 (2001) 094203-1/4.
[25] A.B. Pippard, The Elements of Classical Thermodynamics, Cambridge University Press, Cambridge, 1964.
[26] M.B. Taylor, G.D. Barrera, N.L. Allan, T.H.K. Barron, W.C. Mackrodt, Comput. Phys. Commun. 109 (1998) 135.
[27] X. Gonze, J.M. Beuken, R. Caracas, F. Detraux, M. Fuchs, G.-M. Rignanese, L. Sindic, M. Verstraete, G. Zerah, F. Jollet, M. Torrent, A. Roy, M. Mikami, Ph. Ghosez, J.Y. Raty, D.C. Allan, Comput. Mater. Sci. 25 (2002) 478.
[28] R.M. Martin, Electronic Structure: Basic Theory and Practical Methods, Cambridge University Press, Cambridge, 2004.
[29] P.H.T. Philipsen, E.J. Baerends, Phys. Rev. B 61 (2000) 1773.
[30] S. Goedecker, M. Teter, J. Hutter, Phys. Rev. B 54 (1996) 1703.
[31] C. Hartwigsen, S. Goedecker, J. Hutter, Phys. Rev. B 58 (1998) 3641.
[32] X. Gonze, Phys. Rev. B 55 (1997) 10337.
[33] X. Gonze, C. Lee, Phys. Rev. B 55 (1997) 10355.
[34] Z.A. Bowden, M. Celli, F. Cilloco, D. Colognesi, R.J. Newport, S.F. Parker, F.P. Ricci, V. Rossi-Albertini, F. Sacchetti, J. Tomkinson, M. Zoppi, Physica B 276–278 (2000) 98.
[35] P.C.H. Mitchell, S.F. Parker, A.J. Ramirez-Cuesta, J. Tomkinson, Vibrational Spectroscopy with Neutrons with Applications in Chemistry, Biology, Material Sciences and Catalysis, World Scientific, Singapore, 2005.
[36] A.J. Ramirez-Cuesta, Comput. Phys. Commun. 157 (2004) 226.
[37] D.K. Smith, H.R. Leider, J. Appl. Crystallogr. 1 (1968) 246.
[38] J.P. Vidal, G. Vidal-Valat, Acta Crystallogr., Sect. B 42 (1986) 131.
[39] D.R. Stephens, E.M. Lilley, J. Appl. Phys. 39 (1968) 117.
[40] C.G. Shull, E.O. Wollan, G.A. Morton, W.L. Davidson, Phys. Rev. 73 (1948) 842.
[41] V.G. Kuznetsov, M.M. Shkrabkina, Zh. Strukt. Khim. 3 (1962) 532.
[42] E. Zintl, A. Harder, Z. Phys. Chem. Abt. B 14 (1931) 265.
[43] E.G. Ponyatovskii, I.O. Bashkin, Z. Phys. Chem. 146 (1985) 137.
[44] D. Gerlich, C.S. Smith, J. Phys. Chem. Solids 35 (1974) 1587.
[45] K. Ghandehari, H. Luo, A.L. Ruoff, Phys. Rev. Lett. 74 (1995) 2264.
[46] Ph. Ghosez, J.-P. Michenaud, X. Gonze, Phys. Rev. B 58 (1998) 5224.
[47] M.H. Brodsky, E. Burstein, J. Phys. Chem. Solids 28 (1967) 1655.
[48] D.Kh. Blatt, N.E. Zein, V.I. Zinenko, J. Phys. 3 (1991) 5515.
[49] A. Shukla, Phys. Rev. B 61 (2000) 13277.